Supplementary Information Files

File name: Supplementary_information.docx
Description: Supplementary Figures, Supplementary Figure Legends, and Supplementary Tables

File name: Supplementary_Data1.xlsx
Description: Clinical metadata and sequencing performed by tumor (Basser cohorts)

File name: Supplementary_Data2.xlsx
Description: Tumor mutational burden, HRD and aneuploidy scores by tumor

File name: Supplementary_Data3.xlsx
Description: Gene set enrichment analysis from whole exome sequencing (mutations and copy number variation)

File name: Supplementary_Data4.xlsx
Description: MutSigCV results from primary and recurrent tumor cohorts

File name: Supplementary_Data5.xlsx
Description: Results from all GISTIC analyses

File name: Supplementary_Data6.xlsx
Description: *PARP1* copy number in primary/recurrent and TCGA cohorts

File name: Supplementary_Data7.xlsx
Description: TCGA tumors by group

File name: Supplementary_Data8.xlsx
Description: Gene set enrichment analysis from RNA sequencing

File name: Supplementary_Data9.xlsx
Description: Gene modules identified by RNA sequencing; Gene Ontology results and Transcription Factor Binding Site Motifs identified in gene modules

File name: Supplementary_Data10.xlsx
Description: Gene fusions (FusionInspector output) involving *MALAT1* and immunoglobulin genes

File name: Supplementary_Data11.xlsx
Description: *BRCA2* isoforms expression by tumor and clinical metadata used for survival analyses; Cox Proportional Hazards models

Supplementary Methods

Construction of Tissue Microarrays (TMAs) containing primary and recurrent tumors

Twenty-three primary and recurrent *BRCA1/2* mutation-associated tumors (a subset of the primary/recurrent cohort used throughout the study) were assembled into three tissue microarrays (TMAs). Each tissue microarray contained 4-11 1mm cores per tumor to account for tumor heterogeneity, including intratumoral, stromal, and lymphocytic-rich areas. TMA blocks were constructed, cut, stained, and imaged at the Pathology Clinical Service Center at the University of Pennsylvania. Normal liver, spleen, and kidney tissue from other patients were included as controls for antibody testing.

Immunohistochemistry (IHC) analysis of PARP1

Immunohistochemistry for PARP1 was performed on each TMA using standard laboratory protocols and the PARP (46D11) Rabbit mAb (Cell Signaling Technology, catalog #9532). Stained slides were imaged for quantification at 20x resolution. PARP1 nuclear positivity was quantified for each core using H-score (0-300 scale), as determined by AN. Hematoxylin and eosin (H&E) staining was used to assess tumor content in parallel; cores with inadequate tumor per H&E were excluded by AN. We calculated an average PARP1 H-score for each tumor for downstream analyses (range 3-10 evaluable cores per tumor).

Co-detection by Indexing (CODEX) coverslip preparation and staining

TMA slides were cut at 5μm and placed on previous coated poly-lysine-l coverslips for CODEX[37]. We used a custom 40-plex breast and ovarian cancer specific antibody panel (see **Supplementary Table 2** for antibody list). CODEX staining was performed according to the manufacturer protocols, with one additional step to reduce background fluorescence[38]. Briefly, tissue coverslips were submerged in bleaching solution (4.5% (w/v) H_2O_2 and 20mM NaOH in PBS) after antigen retrieval. While in solution, slides were incubated between two LED lights

(Aibecy A4 Ultra Bright 25,000 Lux LED Light) for 45min at room temperature (RT). Bleaching solution was then replaced, and tissue coverslips were incubated between lights for an additional 45min at RT. Coverslips were then washed four times in 1x PBS for 3-5 minutes. Lastly, the tissue was placed in staining solution following the manufacturer's protocol.

CODEX Imaging

Imaging was performed using a Leica DMi8 inverted microscope with 4 filter cubes (DAPI: Excitation: 359nm Emission: 457nm; RHOD: Excitation: 551nm, Emission: 573nm, Y5: Excitation: 651, Emission: 671nm; Y7: Excitation: 756nm, Emission: 779nm), equipped with 20x lens (numerical aperture: 0.8) and LAS X3.6.0.20104. Each core was imaged with a 20x immersion objective in a 2x2 tiled acquisition, ~300nm/pixel resolution and 6 z-planes per tile. CIM v1.29.0.364 was used to control Fluidics operation and set up cycle/marker information.

Processing of raw images from CODEX

Raw data were formatted and transferred using CIM version 1.29.0.364. We processed the data in order to perform cropping and stitching, flat field correction, drift-compensation, best focus definition and background subtraction. To remove out-of-focus light, image deconvolution was performed using Microvolution software (Microvolution LLC, California, USA). QPTIFFs were generated using processor v1.8.0.257 – dev. We generated 43-55 images per TMA (one per core), each consisting of 41 channels (40 antibodies plus 1 nuclear stain).

CODEX cell segmentation

Processed data (QPTIFF) was opened in Phenochart version 1.1.0. DAPI sensitivity was adapted in order to select individual core areas to train the segmentation algorithm. QPTIFF was then selected and loaded using InForm version 2.5.1. We adapted cell segmentation settings such as pixel intensity, nuclear component splitting, and expected cell size to detect

cells with that varied in size and shape. To define single cell boundaries, we used three markers to identify tumor (TC) and immune cells (IC) and to distinguish between nuclei, cytoplasm and membrane: nuclear marker (DAPI), CD45 (IC), and PANCK (TC). All segmented areas were visually checked with ImageJ v1.53c to confirm appropriate segmentation.

CODEX marker quantification

We used ImageJ v1.53c with CODEX_MAV (version 1.5.0.8) plugin to visualize individual cores and merge cores by tumor. Samples were gated using CD45 to detect immune cells (IC), PANCK or Cytokeratin14 to detect tumor cells (TC), and Vimentin to detected stromal cells. Individual populations for each patient were then gated on RAD51, PD-1 and CTLA-4 positivity. Additionally, pixel intensity of each marker was determined for each population (normalized counts) using ImageJ MAV version 1.5.0.8. All gated cells of each population (such as PANCK+/RAD51+ cells) were visually assessed using ImageJ MAV. The percentages of RAD51+, CTLA-4+, and PD-1+ cells per population (TC or IC) were calculated using the total cell number of each population. In regards to select RAD51+ cells, we only included cells with a nuclear RAD51 expression <1-2μm. We visualized groupwise percentages of cells with box plots generated with GraphPad Prism 6.0. Groupwise differences were assessed using two-sided Wilcoxon rank sum tests (α=0.05).

Supplementary Tables

Supplementary Table 1: Genes included in targeted capture for high-depth sequencing, by coverage type.

Exons+UTR Coverage				Whole Gene Coverage	
ABL1	DICER1	MAP2K2	RAD51	ABCB1	TGFBR2
AKT1	DIRAS3	MAP2K4	RAD51B	APC	TOP2B
AKT2	DLEC1	MAP3K4	RAD51C	ATXN3	TP53
AKT3	DPH1	MAPK1	RAD51D	BRCA1	TSC1
ALK	EIF5A2	MAPK3	RAD52	BRCA2	TSC2
AQR	EME1	MECOM	RAD54B	CCNE1	XRCC1
ARAF	EME2	MET	RAD54L	CDH1	
ARID1A	EPHA3	MLH1	RASSF1	CHD4	
ARL11	ERBB2	MPL	RFC1	CUL4B	
ATM	ERBB3	MRE11A	RNF111	EGFR	
ATR	ERBB4	MSH3	RP11-554I8.2	EP300	
AURKA	ERCC2	MSH4	RP3-510D11.2	FGFR2	
BAP1	ERCC3	MSH6	RPA1	FGFR3	
BARD1	ERCC4	MTOR	RPA2	FLT4	
BLM	ERCC6	MUS81	RPA3	FOXA1	
BRAF	ESR1	NBN	RPA4	GATA3	
BRIP1	FANCA	NF2	RPS6KA2	JAK1	
C11ORF80	FANCE	NOTCH2	RSF1	MAD2L2	
CBX2	FANCM	NOTCH3	SETMAR	MAP3K1	
CCND1	FBXW7	NRAS	SHFM1	MDM2	
CCND2	FGF1	OPCML	SLX4	MSH2	
CCND3	FGFR1	PALB2	SMAD2	MYC	
CDK12	FLT3	PAX8	SMARCA4	NCOR1	
CDK4	FOXL2	PEG3	SMARCB1	NF1	
CDK6	FRS2	PIK3R1	SMCHD1	NOTCH1	
CDKN1A	GNA11	PLAGL1	SPARC	PARP1	
CDKN1B	GNAQ	PMS2	SRC	PARP2	
CDKN1C	GNAS	POLD1	SSBP1	PDGFRA	
CDKN2A	GTF2H3	POLD2	STK11	PIK3CA	
CDKN2B	HRAS	POLD3	TERT	POLE	
CEBPA	IGF1R	POLD4	TOP2A	POLR2A	
CHEK1	JAK2	POLK	TOP3A	PRDM7	
CHEK2	JAK3	PPIE	TOP3B	PTEN	
CREBBP	JARID2	PPM1D	TP53BP1	RAD23B	
CRKL	KDR	PPP2R1A	TRIP13	RAF1	
CSF1R	KIT	PRDM9	WWOX	RB1	
CTNNB1	KLHDC3	PRKCI	XRCC2	RBBP8	
CUL4A	KMT2C	PRKDC	XRCC3	RIC8A	
DAB2	KRAS	PRPF19	XRCC6	RIF1	
DDB1	LIG3	RAB25		SMAD4	
DDR2	MAP2K1	RAD50		TBX3	

Supplementary Table 2: Antibodies conjugated for CODEX.

Antibody	Clone	Manufacturer
TBET	EPR9302	Abcam
Estrogen	SIG3670	Biolegend
PARP1	A6.4.12	Abcam
pATM	EP1890Y	Abcam
Geminin	EPR14637	Abcam
PD-L1	E1L3N	Cell Signaling
TMEM173	SP338	Abcam
RAD51	EPR4030(3)	Abcam
TP63	W15093A	Biolegend
HER2	e2-4001	Invitrogen
yH2AX	2F3	Biolegend
Cytokeratin 17	W16131A	Biolegend
PR	YR85	Abcam
FOXP3	236A/E7	Invitrogen
CD163	EDHu-1	Novus
PD-1	D4W2J	Cell Signaling
BRCA1	MS110	Abcam
Cytokeratin 8	1E8	Biolegend
HLA-DR	EPR3692	Abcam
CTLA-4	EPR1476	Abcam
CD45	2B11+PD7/26	Novusbio
Keratin 5	Poly19055	Biolegend
Vimentin	RV202	BD Pharmingen

Supplementary Figures and Figure Legends

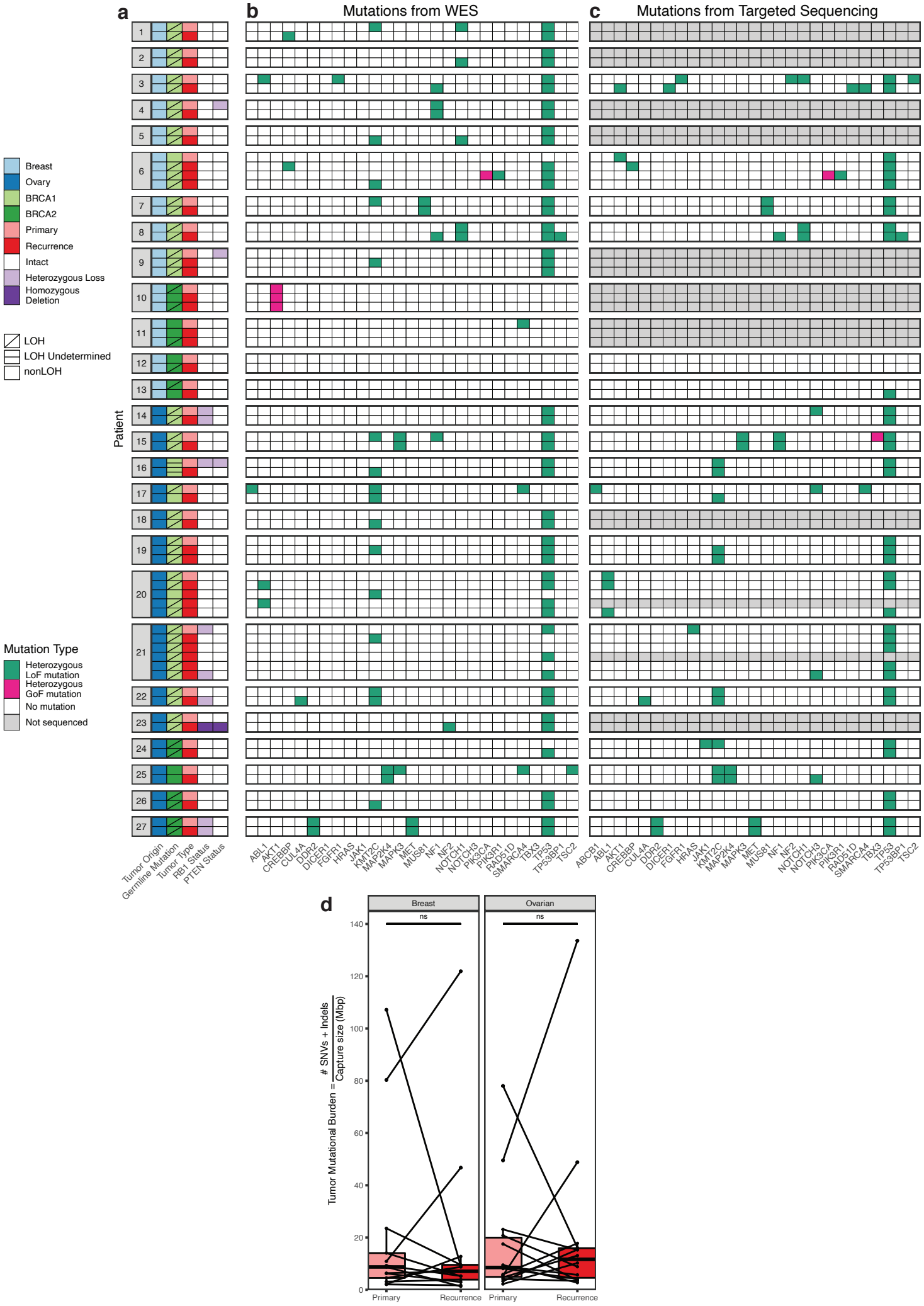
a
b
Mutations from WES
c
Mutations from Targeted Sequencing
Patient
Breast
Ovary
BRCA1
BRCA2
Primary
Recurrence
Intact
Heterozygous Loss
Homozygous Deletion
LOH
LOH Undetermined
nonLOH
Mutation Type
Heterozygous LoF mutation
Heterozygous GoF mutation
No mutation
Not sequenced
Tumor Origin
Germline Mutation
Tumor Type
RB1 Status
PTEN Status
ABL1
AKT1
CREBBP
CUL4A
DDR2
DICER1
FGFR1
HRAS
JAK1
KMT2C
MAP2K4
MAPK3
MET
MUS81
NF1
NF2
NOTCH1
NOTCH3
PIK3CA
PIK3R1
RAD51D
SMARCA4
TBX3
TP53
TP53BP1
TSC2
ABCB1
d
Breast
Ovarian
ns
Tumor Mutational Burden = # SNVs + Indels / Capture size (Mbp)
0
20
40
60
80
100
120
140
Primary
Recurrence

Supplementary Figure 1. Stratified analysis of mutations from whole exome and targeted sequencing. A. 67 paired primary and recurrent tumors from 27 patients sequenced by whole exome sequencing (WES, n=67) and high-depth targeted sequencing (n=44). Tumors are displayed in chronological order by patient, with the primary tumor at the top and latest recurrence at the bottom. B. Somatic mutations from WES, by mutation type and zygosity. C. Somatic mutations from targeted sequencing, by mutation type and zygosity. Display in B and C is limited to genes with $\geq$ 1 mutation with alternative allele fraction $\geq$0.05 from targeted sequencing. D. Comparison of tumor mutational burden for primary/recurrent tumor pairs. For patients with multiple recurrences, one recurrence was chosen at random for comparison. Pairwise differences were determined by two-sided Wilcoxon signed rank test (α=0.05).

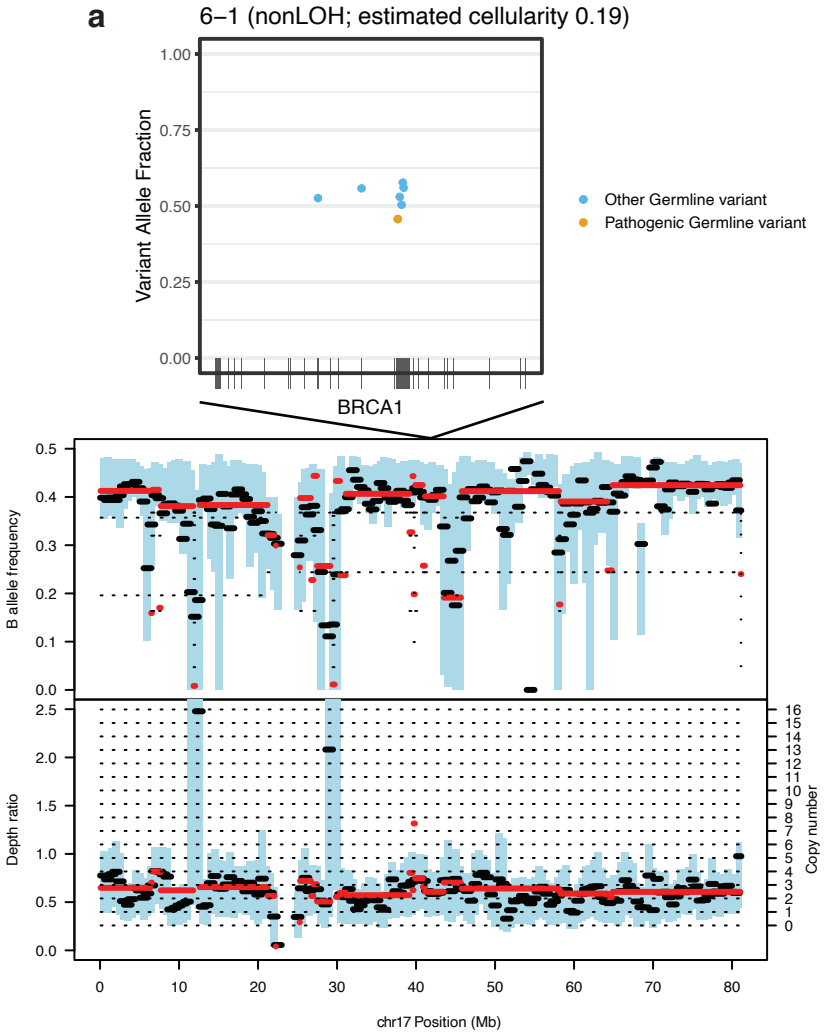
a
6–1 (nonLOH; estimated cellularity 0.19)
Variant Allele Fraction
1.00
0.75
0.50
0.25
0.00
Other Germline variant
Pathogenic Germline variant
BRCA1
B allele frequency
0.5
0.4
0.3
0.2
0.1
0.0
Depth ratio
2.5
2.0
1.5
1.0
0.5
0.0
Copy number
16
15
14
13
12
11
10
9
8
7
6
5
4
3
2
1
0
0
10
20
30
40
50
60
70
80
chr17 Position (Mb)

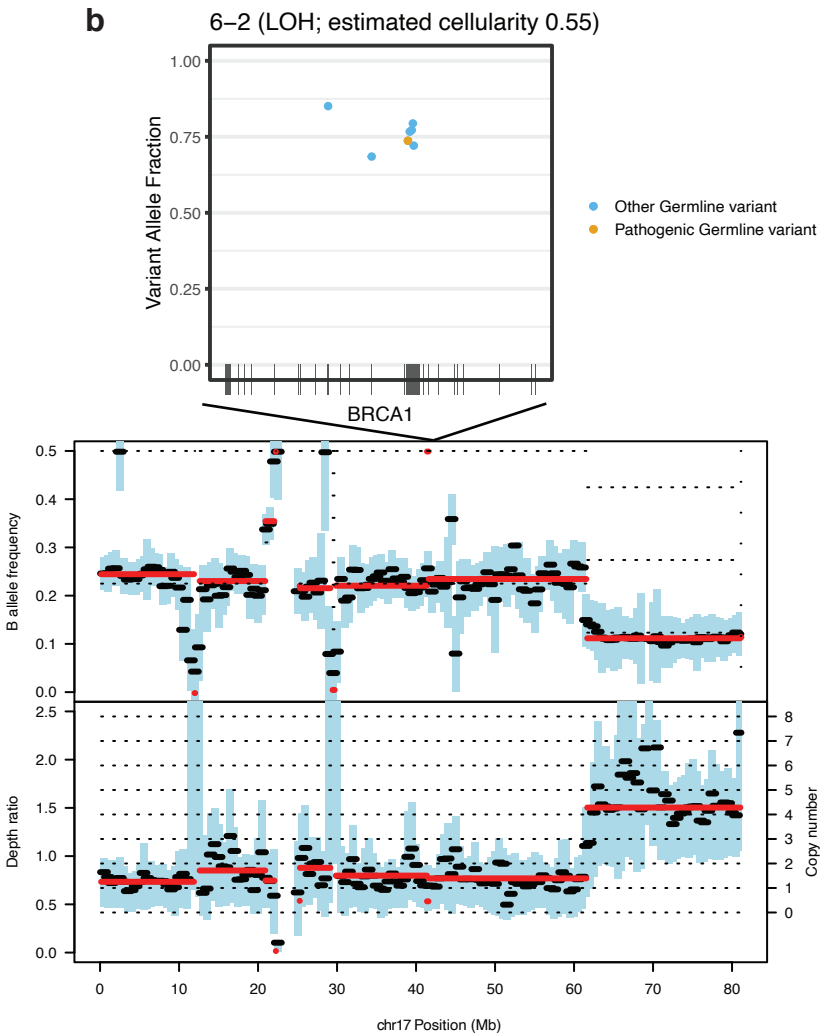
b
6–2 (LOH; estimated cellularity 0.55)
Variant Allele Fraction
1.00
0.75
0.50
0.25
0.00
Other Germline variant
Pathogenic Germline variant
BRCA1
B allele frequency
0.5
0.4
0.3
0.2
0.1
0.0
Depth ratio
2.5
2.0
1.5
1.0
0.5
0.0
Copy number
8
7
6
5
4
3
2
1
0
0
10
20
30
40
50
60
70
80
chr17 Position (Mb)

Supplementary Figure 2. *BRCA1* germline variants, B allele frequency, and copy number before and after a representative nonLOH to LOH transition. A. Location and variant allele fraction of *BRCA1* germline variants in Patient 6's primary breast tumor without LOH (top), pictured with B allele frequency and copy number across chromosome 17 (bottom). B. Location and variant allele fraction of *BRCA1* germline variant in Patient 6's first breast tumor recurrence with LOH (top), pictured with B allele frequency and copy number across chromosome 17 (bottom). For A and B, germline variants were called by VarDictJava and VarScan2. B allele frequency and copy number plots were generated in Sequenza.

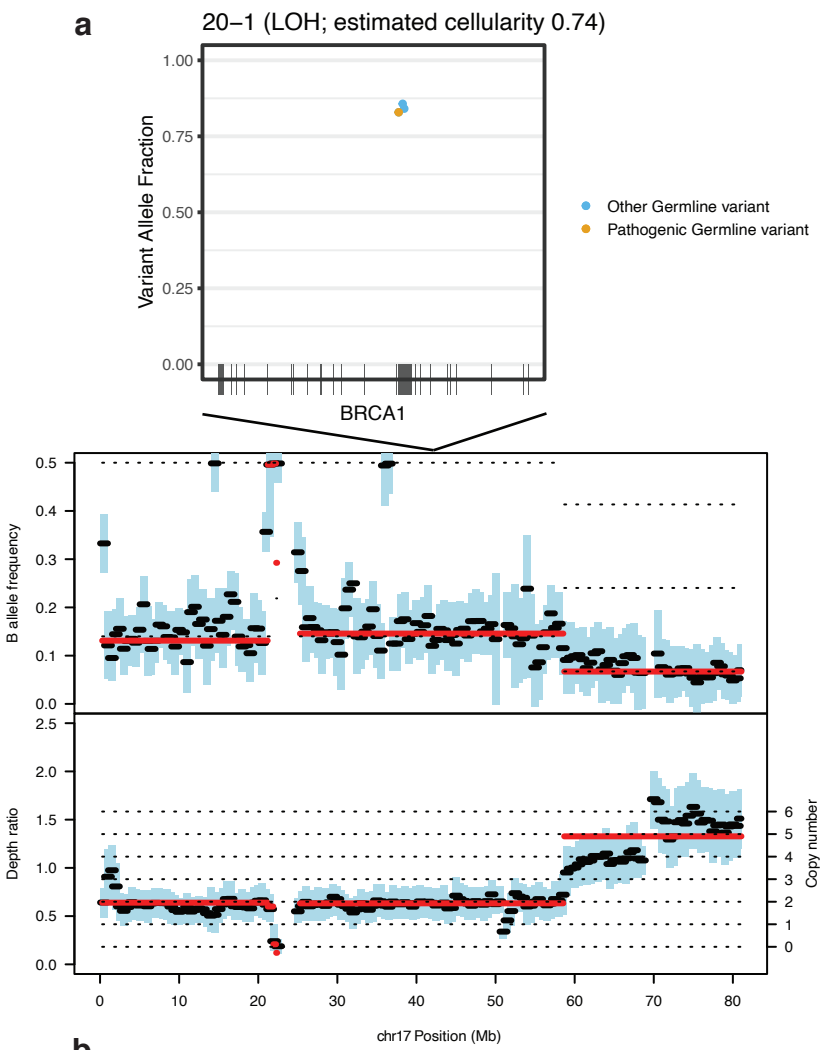
a
20–1 (LOH; estimated cellularity 0.74)
Variant Allele Fraction
1.00
0.75
0.50
0.25
0.00
Other Germline variant
Pathogenic Germline variant
BRCA1
B allele frequency
Depth ratio
Copy number
chr17 Position (Mb)

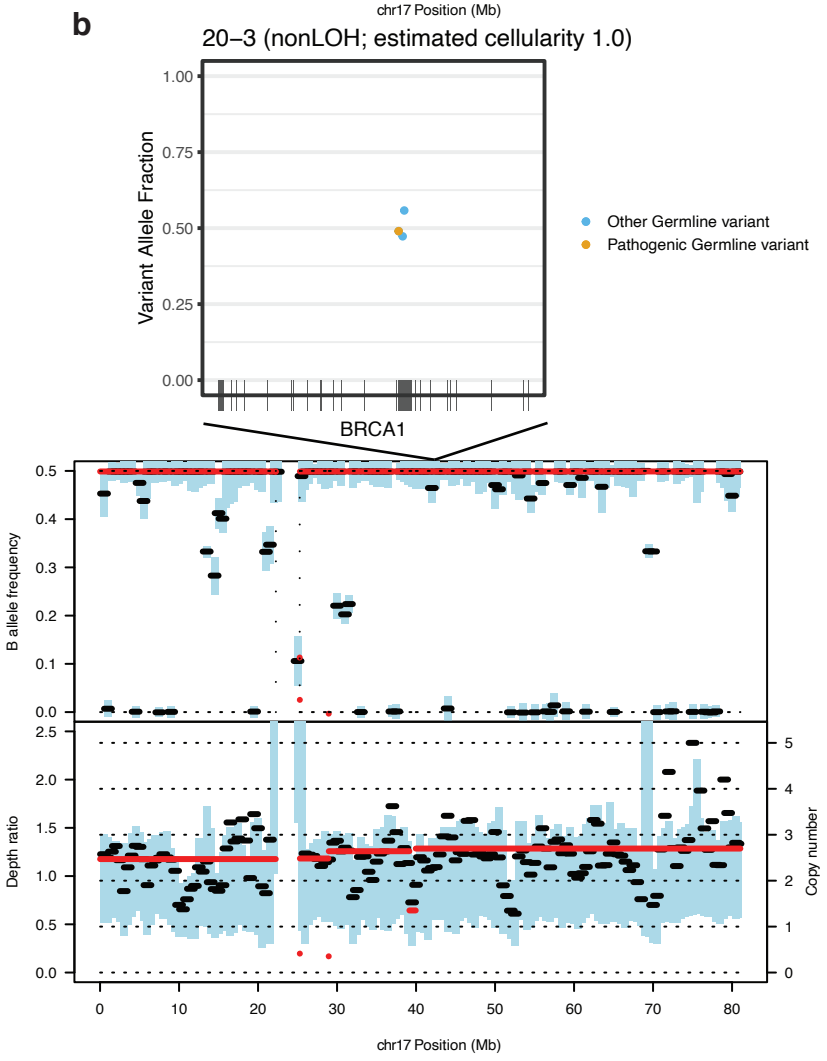
b
20–3 (nonLOH; estimated cellularity 1.0)
Variant Allele Fraction
1.00
0.75
0.50
0.25
0.00
Other Germline variant
Pathogenic Germline variant
BRCA1
B allele frequency
Depth ratio
Copy number
chr17 Position (Mb)

Supplementary Figure 3. *BRCA1* germline variants, B allele frequency, and copy number before and after a representative LOH reversal. A. Location and variant allele fraction of *BRCA1* germline variants in Patient 20's primary ovarian tumor with LOH (top), pictured with B allele frequency and copy number across chromosome 17 (bottom). B. Location and variant allele fraction of *BRCA1* germline variant in Patient 20's second ovarian tumor recurrence without LOH (top), pictured with B allele frequency and copy number across chromosome 17 (bottom). For A and B, germline variants were called by VarDictJava and VarScan2. B allele frequency and copy number plots were generated in Sequenza.

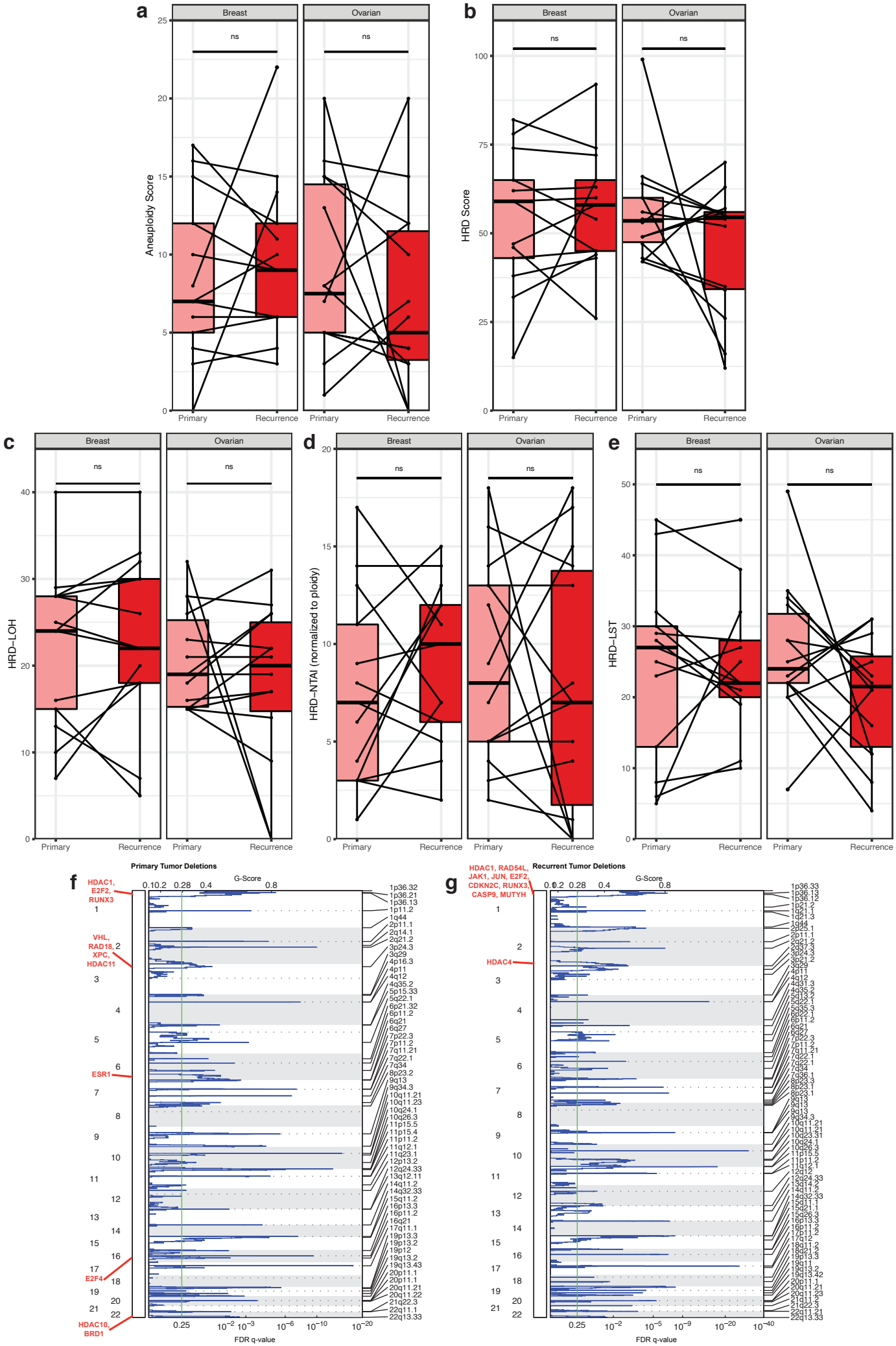
a
Breast
Ovarian
ns
Aneuploidy Score
Primary
Recurrence
b
HRD Score
c
HRD−LOH
d
HRD−NTAI (normalized to ploidy)
e
HRD−LST
f
Primary Tumor Deletions
G-Score
HDAC1, E2F2, RUNX3
VHL, RAD18, XPC, HDAC11
ESR1
E2F4
HDAC10, BRD1
FDR q-value
g
Recurrent Tumor Deletions
HDAC1, RAD54L, JAK1, JUN, E2F2, CDKN2C, RUNX3, CASP9, MUTYH
HDAC4

Supplementary Figure 4. Genome-wide measures of copy number variation in primary/recurrent cohort. A. Comparison of aneuploidy score for primary/recurrent tumor pairs. B. Comparison of HRD score for primary/recurrent tumor pairs. C-E. Comparison of individual HRD metrics for primary/recurrent tumor pairs: loss of heterozygosity (C), non-telomeric allelic imbalance (D), and large scale state transitions (E). For patients with multiple recurrences, one recurrence was chosen at random for statistical comparisons in plots A-E. Pairwise differences were determined by two-sided Wilcoxon signed rank test (α=0.05). F. GISTIC qplot for 90% confidence interval deletions in primary tumors. G. GISTIC qplot for 90% confidence interval deletions in recurrences. For F and G, all highlighted genes have residual q<0.05.

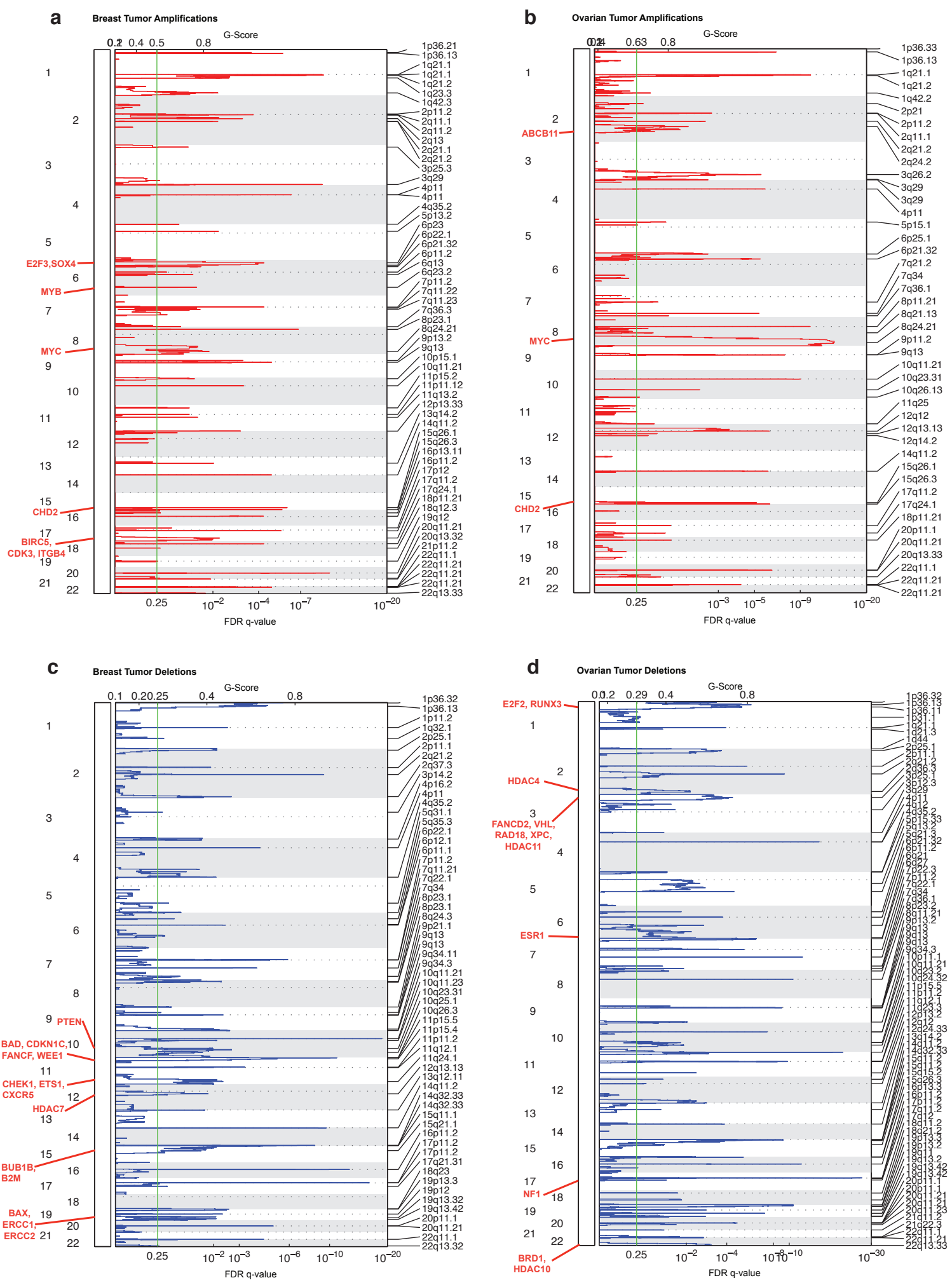
a
Breast Tumor Amplifications
G-Score
FDR q-value
E2F3,SOX4
MYB
MYC
CHD2
BIRC5, CDK3, ITGB4
b
Ovarian Tumor Amplifications
G-Score
FDR q-value
ABCB11
MYC
CHD2
c
Breast Tumor Deletions
G-Score
FDR q-value
PTEN
BAD, CDKN1C, FANCF, WEE1
CHEK1, ETS1, CXCR5
HDAC7
BUB1B, B2M
BAX, ERCC1, ERCC2
d
Ovarian Tumor Deletions
G-Score
FDR q-value
E2F2, RUNX3
HDAC4
FANCD2, VHL, RAD18, XPC, HDAC11
ESR1
NF1
BRD1, HDAC10

Supplementary Figure 5. GISTIC results by tumor type in primary/recurrent cohort. A. GISTIC qplot for 90% confidence interval amplifications in (primary and recurrent) breast tumors. B. GISTIC qplot for 90% confidence interval amplifications in (primary and recurrent) ovarian tumors. C. GISTIC qplot for 90% confidence interval deletions in (primary and recurrent) breast tumors. D. GISTIC qplot for 90% confidence interval deletions in (primary and recurrent) ovarian tumors. For A-D, all highlighted genes have residual $q<0.05$.

a

TCGA PanCancer Breast and Ovarian patients with matched tumor/normal WES
n=864 breast
n=327 ovarian

Remove tumors that failed QC
n=6 breast
n=15 ovarian

Identify tumors with a pathogenic germline mutation in *BRCA1* or *BRCA2* (see **Methods**)

BRCA1/2 germline mutation-associated tumors (g*BRCA1/2* group)
n=37 Breast
n=69 Ovarian

For tumors without g*BRCA1/2* mutation: Remove tumors with somatic *BRCA1/2* loss via somatic mutation, deletion, low expression, or *BRCA1* promoter methylation (see **Methods**)
n=44 breast
n=35 ovarian

Remove tumors with germline or somatic mutations in HR-related genes (see **Supplementary File 7**)
n=119 breast
n=9 ovarian

Tumors proficient for homologous recombination genes (HR-WT group)
n=657 Breast
n=198 Ovarian

Remove tumors that failed Sequenza
n=1 HR-WT Breast
n=1 g*BRCA1/2* Ovarian

b

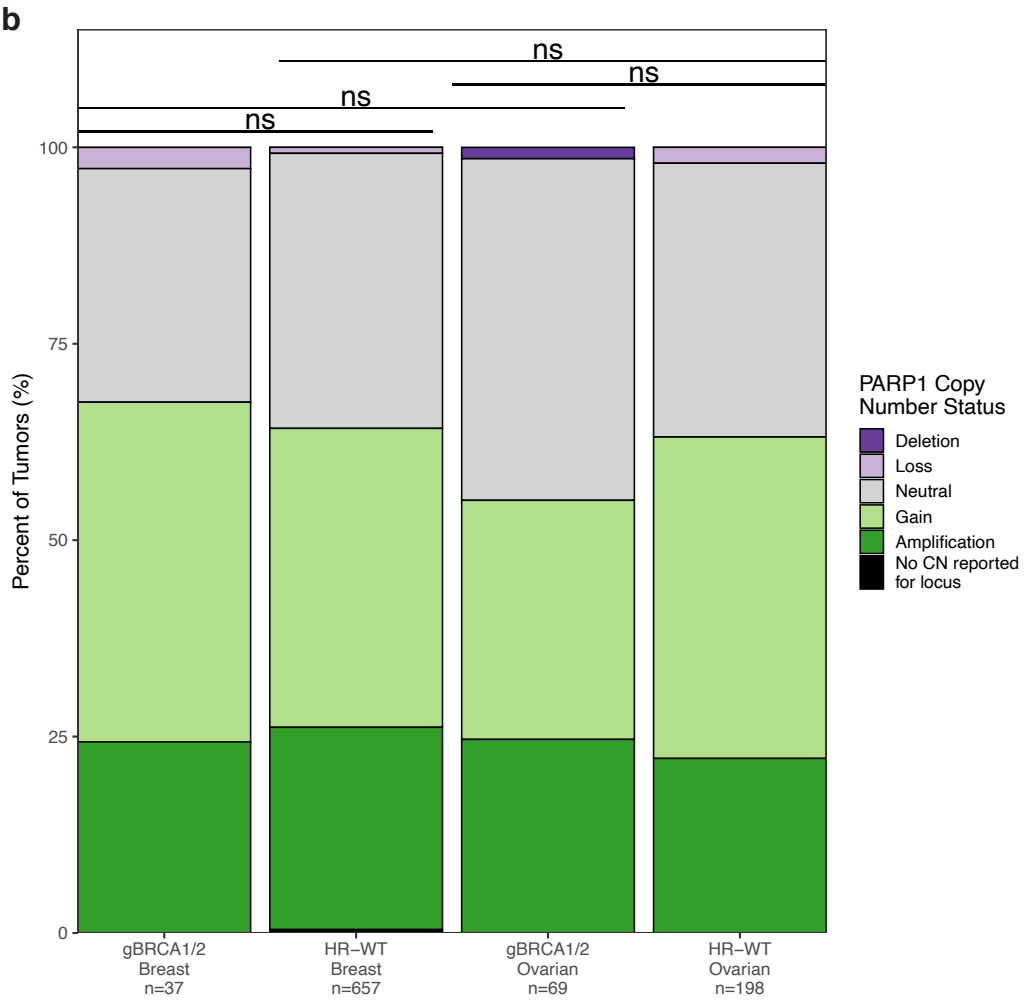

Supplementary Figure 6. Analysis of *PARP1* copy number variation in TCGA cohorts. A. Strategy for grouping TCGA breast and ovarian tumors into g*BRCA1/2* and HR-WT groups for analysis. Tumors were excluded on the basis of somatic *BRCA1/2* loss or mutations in genes required for homologous recombination. B. *PARP1* copy number by tumor in selected TCGA breast and ovarian cohorts. Groupwise differences in average copy number were determined by two-sided t-test (α=0.05). Copy number (Sequenza) was binned as follows: Deletion, CN=0; Loss, CN=1; Neutral, CN=2-3; Gain, CN=4-5; Amplification, CN≥6.

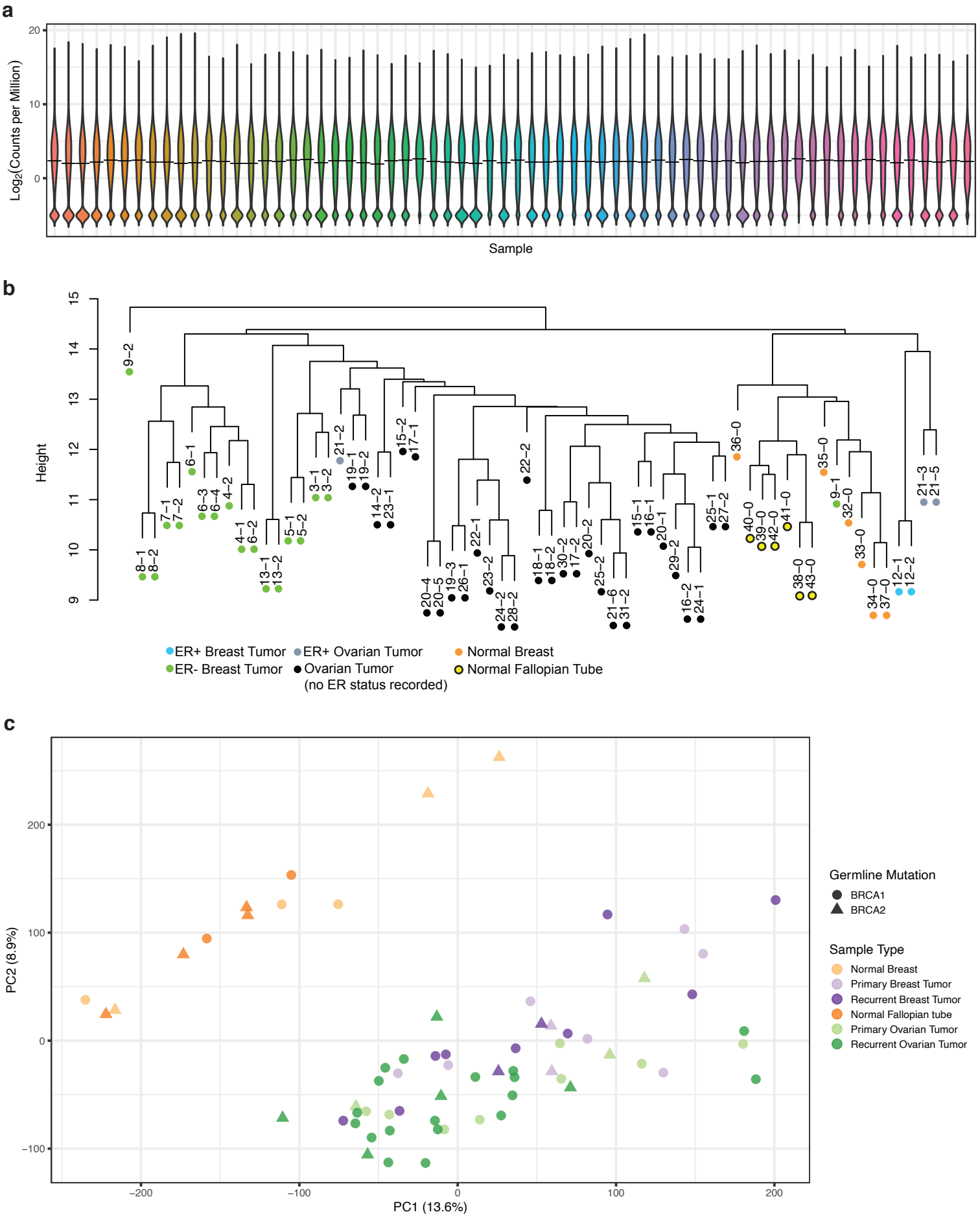
a
Log2(Counts per Million)
Sample
b
Height
ER+ Breast Tumor
ER+ Ovarian Tumor
Normal Breast
ER- Breast Tumor
Ovarian Tumor
(no ER status recorded)
Normal Fallopian Tube
c
PC2 (8.9%)
PC1 (13.6%)
Germline Mutation
BRCA1
BRCA2
Sample Type
Normal Breast
Primary Breast Tumor
Recurrent Breast Tumor
Normal Fallopian tube
Primary Ovarian Tumor
Recurrent Ovarian Tumor

Supplementary Figure 7. Sample relatedness identified by RNA sequencing. A. Distribution of Log_2(counts per million) across cohort of samples used for RNA sequencing. B. Dendrogram of sample relatedness across RNA sequencing cohort, by tumor type and estrogen receptor status. C. Principal components analysis of RNA sequencing cohort.

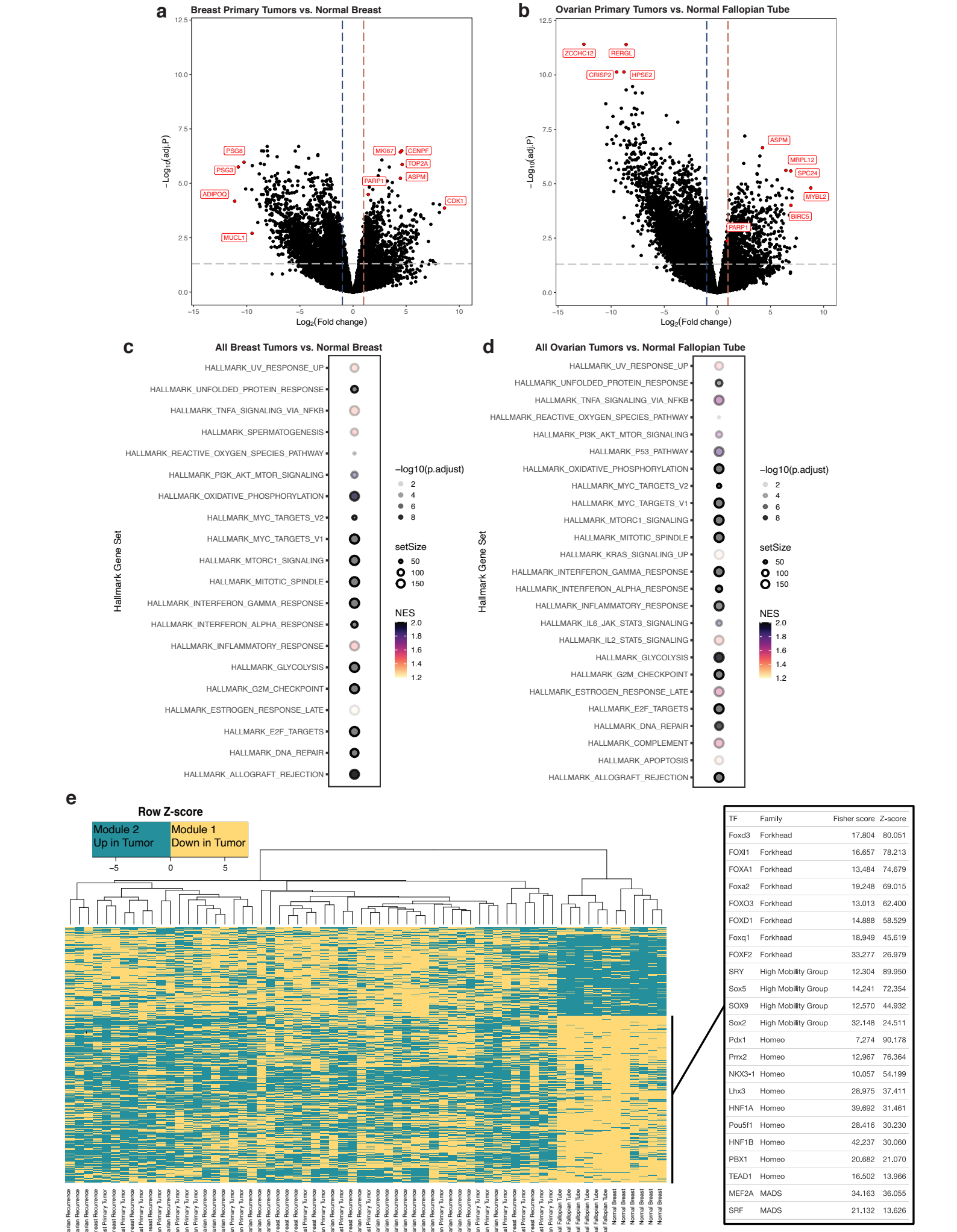

TF	Family	Fisher score	Z-score
Foxd3	Forkhead	17.804	80.051
FOXI1	Forkhead	16.657	78.213
FOXA1	Forkhead	13.484	74.679
Foxa2	Forkhead	19.248	69.015
FOXO3	Forkhead	13.013	62.400
FOXD1	Forkhead	14.888	58.529
Foxq1	Forkhead	18.949	45.619
FOXF2	Forkhead	33.277	26.979
SRY	High Mobility Group	12.304	89.950
Sox5	High Mobility Group	14.241	72.354
SOX9	High Mobility Group	12.570	44.932
Sox2	High Mobility Group	32.148	24.511
Pdx1	Homeo	7.274	90.178
Prrx2	Homeo	12.967	76.364
NKX3-1	Homeo	10.057	54.199
Lhx3	Homeo	28.975	37.411
HNF1A	Homeo	39.692	31.461
Pou5f1	Homeo	28.416	30.230
HNF1B	Homeo	42.237	30.060
PBX1	Homeo	20.682	21.070
TEAD1	Homeo	16.502	13.966
MEF2A	MADS	34.163	36.055
SRF	MADS	21.132	13.626

Supplementary Figure 8. Differential gene expression in tumors vs. normal tissue. A. Differential gene expression in primary breast tumors vs. normal breast tissue from *BRCA1/2* mutation carriers. B. Differential gene expression in primary ovarian tumors vs. normal fallopian tube tissue from *BRCA1/2* mutation carriers. For A and B, a positive Log_2(fold change) indicates genes with increased expression in primary tumors. Adjusted p values were computed based on linear modeling of mean-variance trends (limma). C. Hallmark Gene Sets enriched in genes with increased expression in primary and recurrent breast tumors compared to normal breast tissue from *BRCA1/2* mutation carriers. D. Hallmark Gene Sets enriched in genes with increased expression in primary and recurrent ovarian tumors compared to normal fallopian tube from *BRCA1/2* mutation carriers. For C and D, all gene sets had adj. $p<0.05$. E. Heatmap of hierarchical clustering to identify modules within differentially expressed genes (with adj.$p<0.05$ and $|\log_2 FC|>1$) for tumor vs. normal comparisons. Module of genes with decreased expression in tumor compared to normal tissue (coded yellow on heatmap) were enriched for transcription factor motifs as indicated (all Z-score ≥ 10, Fisher score ≥ 7 for motif enrichment).

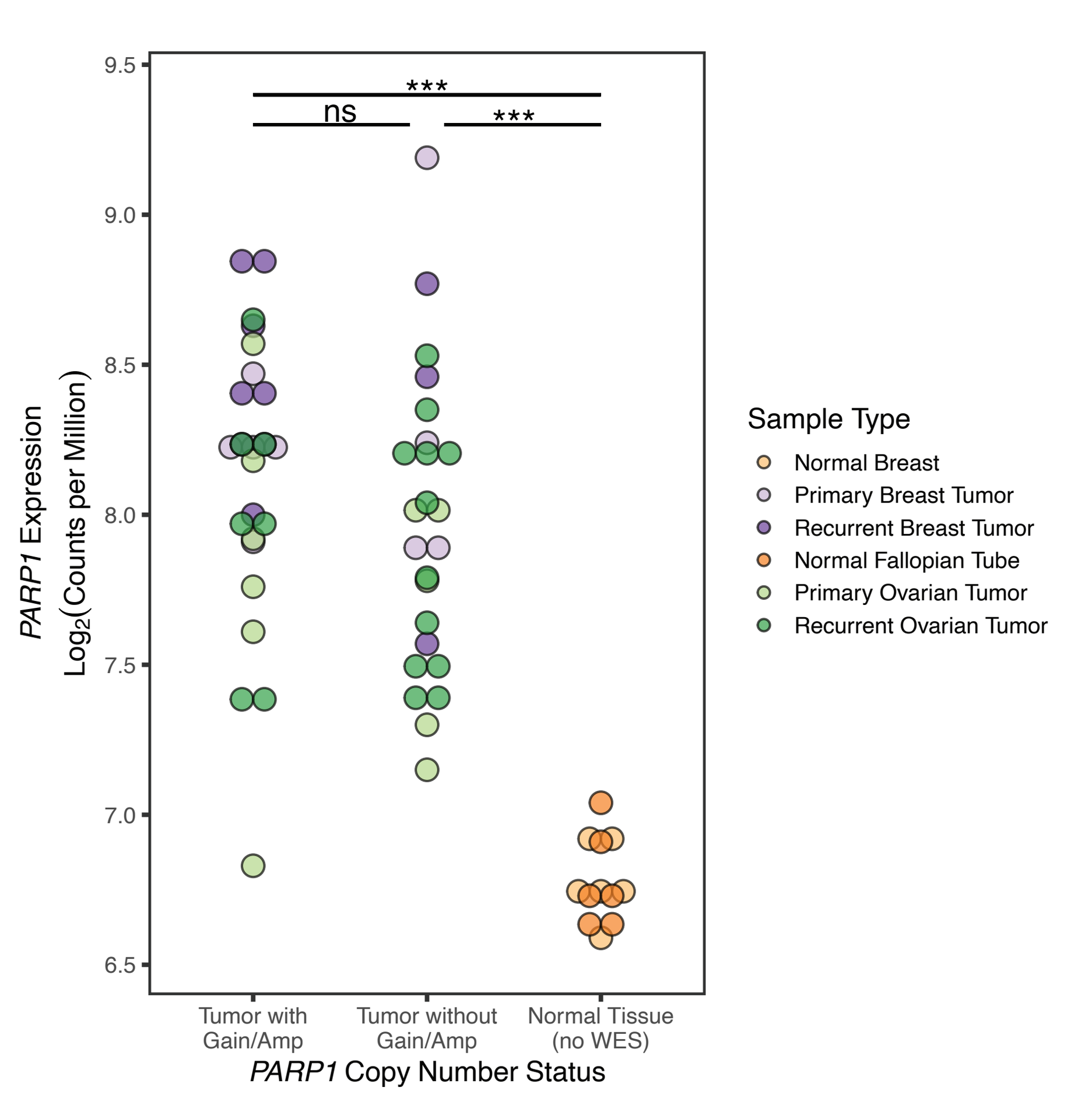
9.5
9.0
8.5
8.0
7.5
7.0
6.5
***
ns
***
PARP1 Expression
Log2(Counts per Million)
Tumor with Gain/Amp
Tumor without Gain/Amp
Normal Tissue (no WES)
PARP1 Copy Number Status
Sample Type
Normal Breast
Primary Breast Tumor
Recurrent Breast Tumor
Normal Fallopian Tube
Primary Ovarian Tumor
Recurrent Ovarian Tumor

Supplementary Figure 9. *PARP1* expression and copy number status in primary and recurrent tumors. *PARP1* copy number status and expression across all tumors with WES and RNA-seq, and all normal samples with RNA-seq. Groupwise differences in average copy number were determined by Kruskal-Wallis test, followed by Dunn's test with Bonferroni correction (α=0.05, ***p<0.0001).

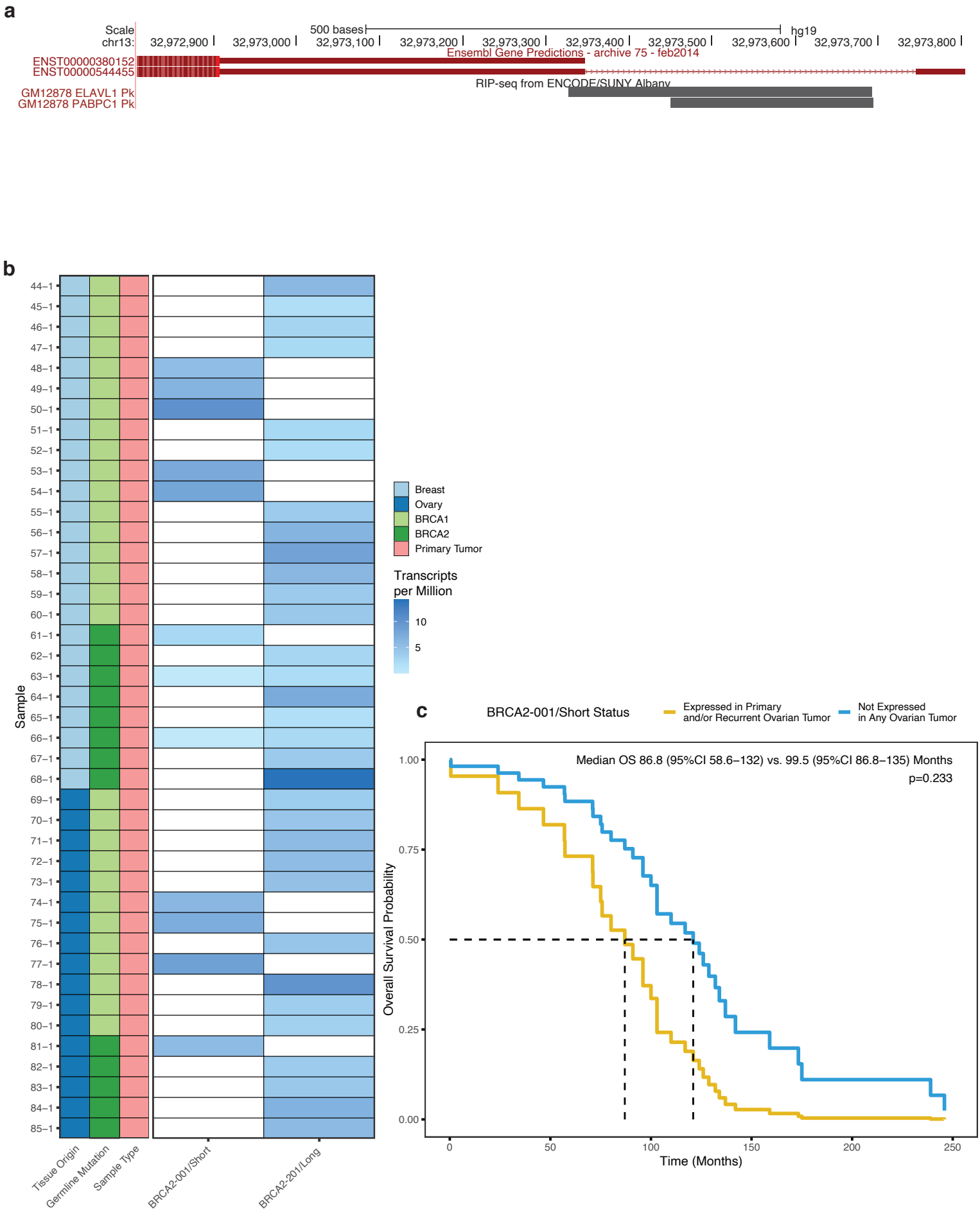
a
Scale
chr13:
500 bases
hg19
32,972,900
32,973,000
32,973,100
32,973,200
32,973,300
32,973,400
32,973,500
32,973,600
32,973,700
32,973,800
Ensembl Gene Predictions - archive 75 - feb2014
ENST00000380152
ENST00000544455
RIP-seq from ENCODE/SUNY Albany
GM12878 ELAVL1 Pk
GM12878 PABPC1 Pk
b
Sample
Breast
Ovary
BRCA1
BRCA2
Primary Tumor
Transcripts per Million
10
5
Tissue Origin
Germline Mutation
Sample Type
BRCA2-001/Short
BRCA2-201/Long
c
BRCA2-001/Short Status
Expressed in Primary and/or Recurrent Ovarian Tumor
Not Expressed in Any Ovarian Tumor
Median OS 86.8 (95%CI 58.6–132) vs. 99.5 (95%CI 86.8–135) Months
p=0.233
Overall Survival Probability
1.00
0.75
0.50
0.25
0.00
0
50
100
150
200
250
Time (Months)

Supplementary Figure 10. Differential isoform usage of *BRCA2* in a validation cohort of *BRCA1/2* mutation-associated primary tumors. A. RNA binding protein (ELAVL1/HuR and PABPC1) prediction for *BRCA2* transcripts based on RNA immunoprecipitation sequencing (RIP-seq) in GM12878 (Human B cells). ENST00000380152 refers to *BRCA2-001/Short*; ENST00000544455 refers to *BRCA2-201/Long*. B. *BRCA2* isoform usage by sample type in an independent cohort of 42 primary breast and ovarian tumors from *BRCA1/2* mutation carriers. C. Survival curve for patients that expressed *BRCA2-001/Short* in any (primary or recurrent) ovarian tumor compared to those that did not. Survival proportions and p-value were calculated using a Cox proportional hazards model tested for significant associations with ER status, age at diagnosis, tumor stage at diagnosis; and adjusted for patient recurrent status (α=0.05, see **Methods**).

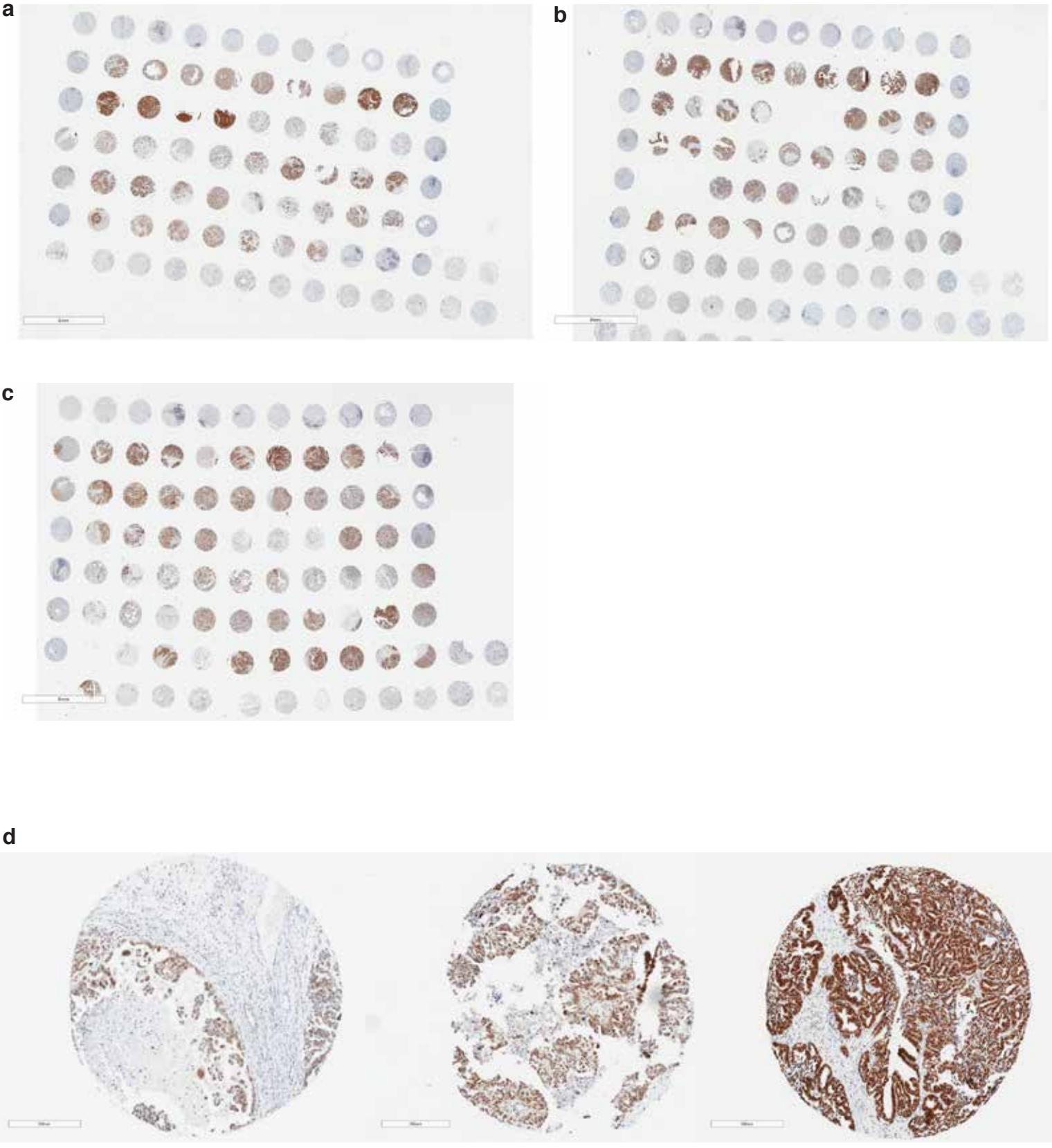
a
b
c
d

Supplementary Figure 11. PARP1 expression in primary/recurrent tumors by immunohistochemistry (IHC). A. Image of PARP1 IHC in tissue microarray (TMA) of primary and recurrent breast tumors. B. Image of PARP1 IHC in TMA of primary and recurrent ovarian tumors (1/2). C. Image of PARP1 IHC in TMA of primary and recurrent ovarian tumors (2/2). For A-C, images were taken at 0.5x magnification. D. Representative images of individual TMA cores from ovarian tumors with low PARP1 expression (left, H-score = 125), medium PARP1 expression (middle, H-score = 200), and high PARP1 expression (right, H-score = 300). Images were taken at 7-7.2x.

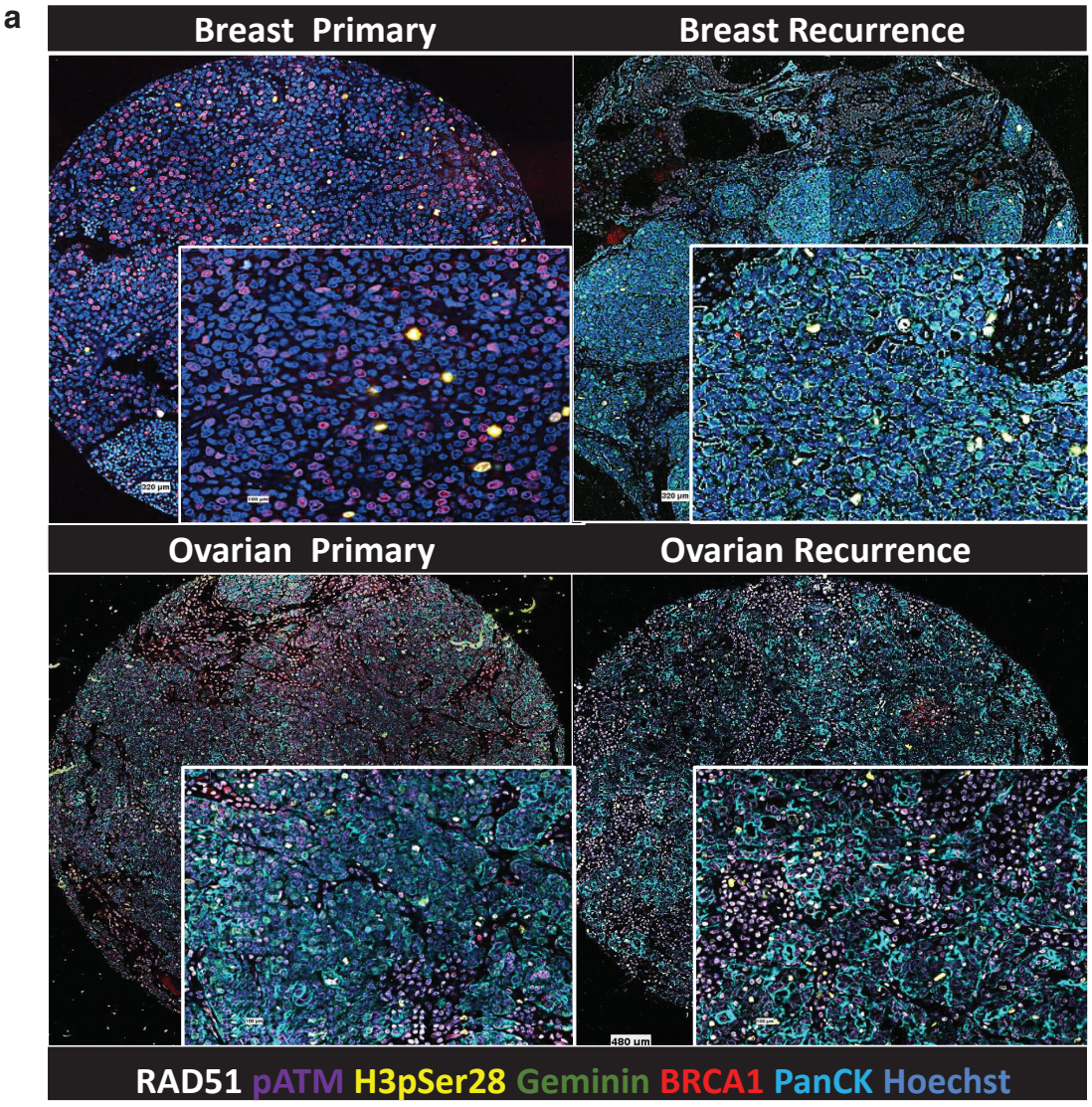
a
Breast Primary
Breast Recurrence
Ovarian Primary
Ovarian Recurrence
320 µm
480 µm
RAD51 pATM H3pSer28 Geminin BRCA1 PanCK Hoechst

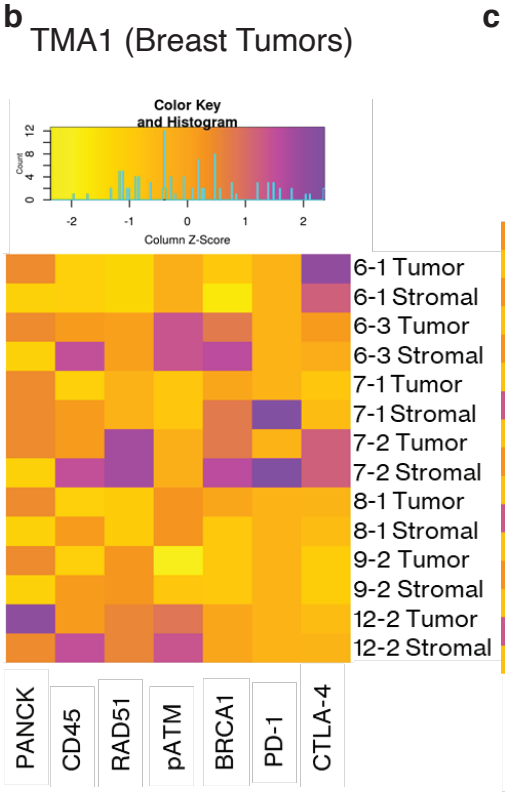
b
TMA1 (Breast Tumors)
Color Key and Histogram
Count
Column Z-Score
6-1 Tumor
6-1 Stromal
6-3 Tumor
6-3 Stromal
7-1 Tumor
7-1 Stromal
7-2 Tumor
7-2 Stromal
8-1 Tumor
8-1 Stromal
9-2 Tumor
9-2 Stromal
12-2 Tumor
12-2 Stromal
PANCK
CD45
RAD51
pATM
BRCA1
PD-1
CTLA-4

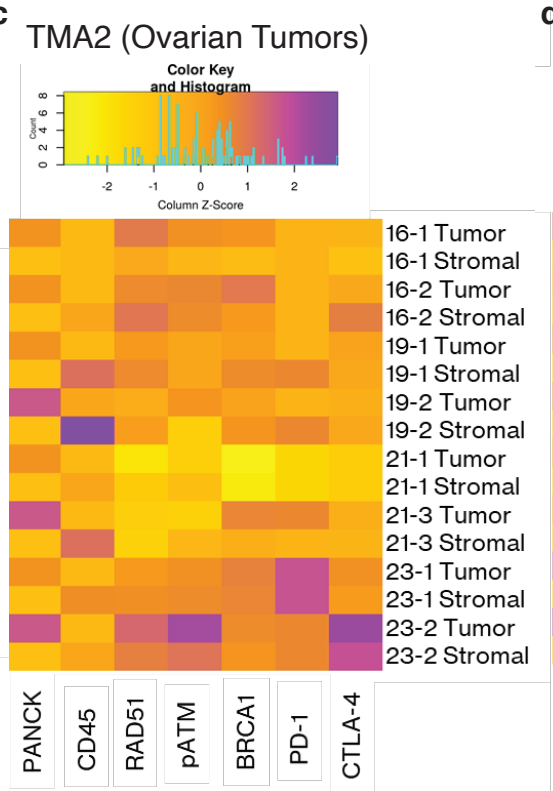
c
TMA2 (Ovarian Tumors)
Color Key and Histogram
Count
Column Z-Score
16-1 Tumor
16-1 Stromal
16-2 Tumor
16-2 Stromal
19-1 Tumor
19-1 Stromal
19-2 Tumor
19-2 Stromal
21-1 Tumor
21-1 Stromal
21-3 Tumor
21-3 Stromal
23-1 Tumor
23-1 Stromal
23-2 Tumor
23-2 Stromal
PANCK
CD45
RAD51
pATM
BRCA1
PD-1
CTLA-4

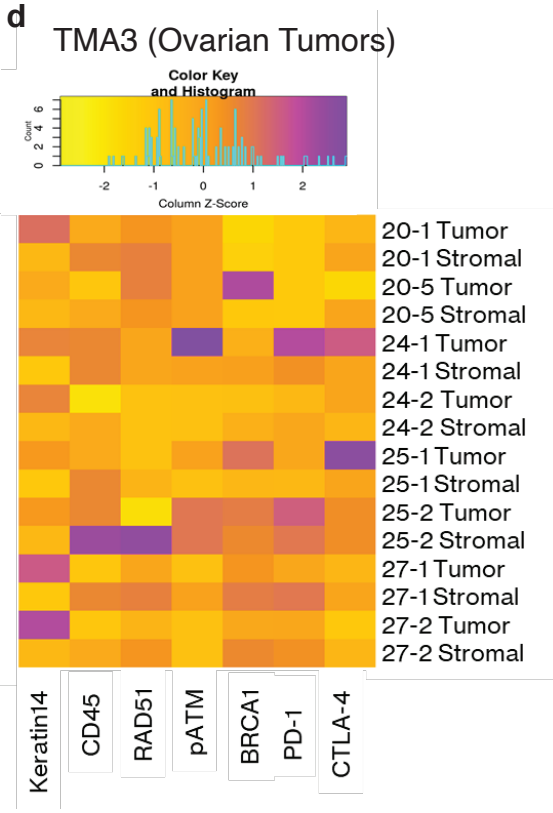
d
TMA3 (Ovarian Tumors)
Color Key and Histogram
Count
Column Z-Score
20-1 Tumor
20-1 Stromal
20-5 Tumor
20-5 Stromal
24-1 Tumor
24-1 Stromal
24-2 Tumor
24-2 Stromal
25-1 Tumor
25-1 Stromal
25-2 Tumor
25-2 Stromal
27-1 Tumor
27-1 Stromal
27-2 Tumor
27-2 Stromal
Keratin14
CD45
RAD51
pATM
BRCA1
PD-1
CTLA-4

Supplementary Figure 12. Comparisons of DNA damage markers and immune checkpoint proteins in paired primary/recurrent tumors by CODEX. A. Representative image of cell cycle and DNA damage markers in breast and ovarian primary and recurrent tumors. B. Expression of markers for cell type, DNA damage response, and immune checkpoints in primary and recurrent breast tumors from five patients. C. Expression of markers for cell type, DNA damage response, and immune checkpoints in primary and recurrent ovarian tumors from four patients. D. Expression of markers for cell type, DNA damage response, and immune checkpoints in primary and recurrent ovarian tumors from four additional patients. For B-D, tumor and stromal cells are displayed separately for each specimen; PANCK, Keratin14, and CD45 were used for gating of tumor and stroma (see **Supplementary Methods**). Tumors are numbered in chronological order following the convention [Patient] - [Tumor number] such that 16-1 is Patient 16's primary tumor, 16-2 the first recurrence, etc. For clinical metadata from individual tumors, see **Supplementary Data 1**.

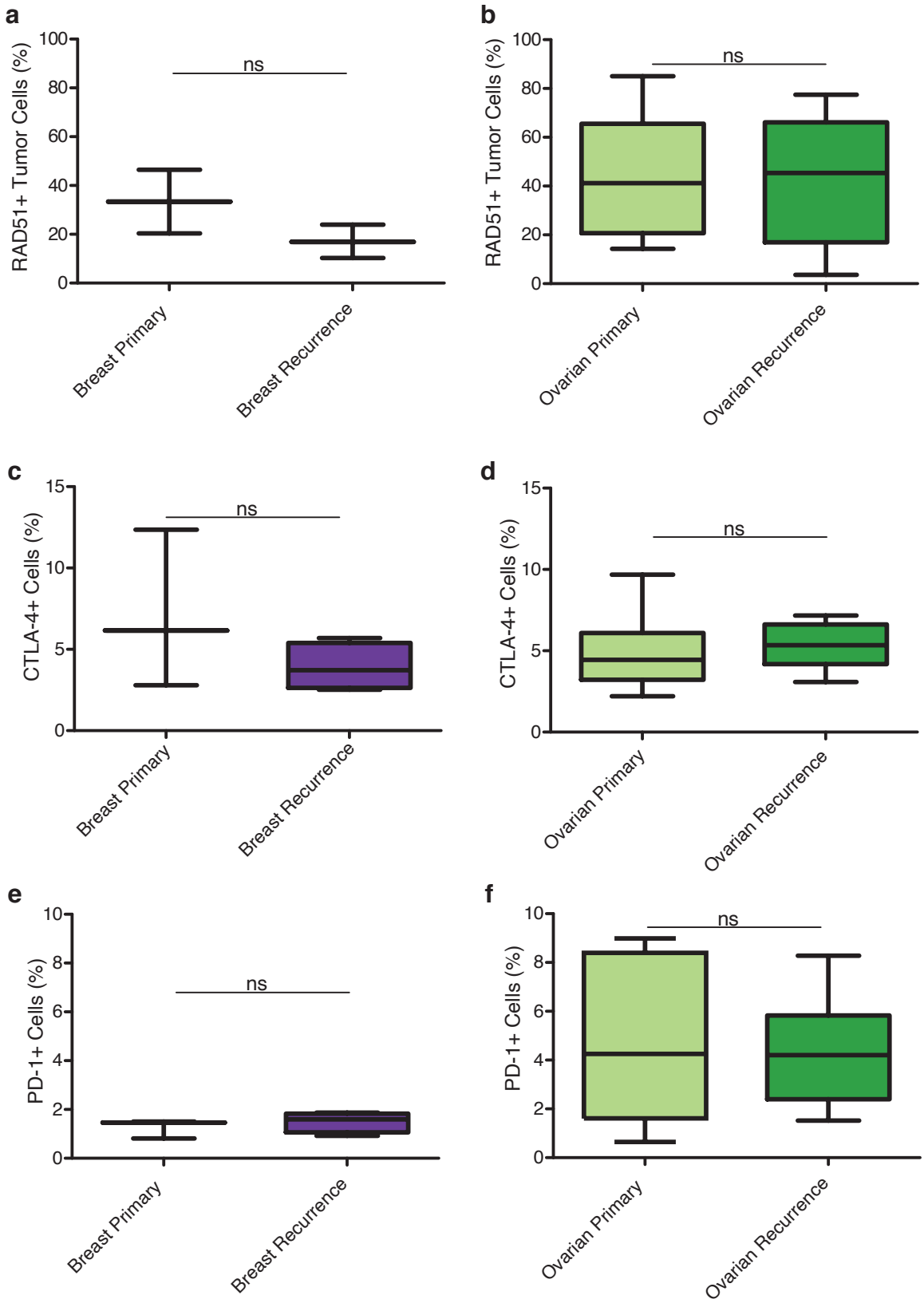
a
RAD51+ Tumor Cells (%)
100
80
60
40
20
0
ns
Breast Primary
Breast Recurrence
b
RAD51+ Tumor Cells (%)
100
80
60
40
20
0
ns
Ovarian Primary
Ovarian Recurrence
c
CTLA-4+ Cells (%)
15
10
5
0
ns
Breast Primary
Breast Recurrence
d
CTLA-4+ Cells (%)
15
10
5
0
ns
Ovarian Primary
Ovarian Recurrence
e
PD-1+ Cells (%)
10
8
6
4
2
0
ns
Breast Primary
Breast Recurrence
f
PD-1+ Cells (%)
10
8
6
4
2
0
ns
Ovarian Primary
Ovarian Recurrence

Supplementary Figure 13. Comparisons of RAD51 and immune checkpoint protein expression in primary and recurrent tumors by CODEX. A. Percent of RAD51+ tumor cells in primary vs. recurrent breast tumors. B. Percent of RAD51+ tumor cells in primary vs. recurrent ovarian tumors. C. Percent of CTLA-4+ cells in primary vs. recurrent breast tumors. D. Percent of CTLA-4+ cells in primary vs. recurrent ovarian tumors. E. Percent of PD-1+ cells in primary vs. recurrent breast tumors. F. Percent of PD-1+ cells in primary vs. recurrent ovarian tumors. For A-F, sample sizes were as follows: n=3 primary breast tumors, n=4 recurrent breast tumors, n=8 primary ovarian tumors, n=8 recurrent ovarian tumors. Groupwise differences were determined by two-sided Wilcoxon rank sum test (α=0.05).


a
BRCA1 germline mutation
A T G C G A C T
Somatic reversion mutation
(in-frame deletion)
b
41,243,460 bp
41,243,470 bp
41,243,480 bp
41,243,490 bp
T T T G A A T C C A T G C T T T G C T C T T C T T G A T T A T T T T C T T C C
Patient 20 Germline
BRCA1 c.G4069T
Pt 20 Primary Ovarian Tumor
Pt 20 Recurrence 1
Pt 20 Recurrence 2
Pt 20 Recurrence 3
Pt 20 Recurrence 4
Refseq Genes
BRCA1
BRCA1

Supplementary Figure 14. Somatic reversion of *BRCA1* after PARPi in Patient 20. A. Graphical representation of in-frame somatic deletion of germline nonsense mutation in *BRCA1* (mutation pictured is not Patient 20's actual germline mutation). B. IGV tracks from WES of germline and tumor DNA from patient 20. For each sample, forward strand alignment and coverage tracks are displayed around the site of the patient's germline *BRCA1* c.G4069T (p.E1357X) mutation. G>T mutation appears as C>A because *BRCA1* lies on reverse strand.